

Large effects on $B_s\bar{B}_s$ mixing by vectorlike quarks

Mayumi Aoki,¹ Gi-Chol Cho,² Makiko Nagashima,³ and Noriyuki Oshimo²

¹Theory Group, KEK, Tsukuba, Ibaraki 305-0801, Japan

²Department of Physics, Ochanomizu University, Bunkyo-ku, Tokyo 112-8610, Japan

³Graduate School of Humanities and Sciences, Ochanomizu University, Bunkyo-ku, Tokyo 112-8610, Japan

(Received 5 July 2001; published 13 November 2001)

We calculate the contributions of the vectorlike quark model to $B_s\bar{B}_s$ mixing, taking into account the constraints from the decay $B \rightarrow X_s \gamma$. In this model the neutral bosons mediate flavor-changing interactions at the tree level. However, $B_s\bar{B}_s$ mixing is dominated by contributions from the box diagrams with the top quark and the extra up-type quark. In sizable ranges of the model parameters, the mixing parameter x_s is much different from the standard model prediction.

DOI: 10.1103/PhysRevD.64.117305

PACS number(s): 12.15.Ff, 12.60.-i, 14.40.Nd

The standard model (SM) may have to be extended to describe physics around or above the electroweak scale. Various works have thus discussed phenomena involving the B meson which are sensitive to new physics [1]. For instance, the radiative B -meson decay $B \rightarrow X_s \gamma$ and $B\bar{B}$ mixing could receive nontrivial contributions from supersymmetry [2,3]. The vectorlike quark model (VQM) could also affect these processes of flavor-changing neutral currents [4,5].

In this Brief Report we discuss $B_s\bar{B}_s$ mixing within the framework of the VQM which is one of the minimal extensions of the SM. The mixing parameter x_s is evaluated and its dependencies on the model parameters are analyzed. These model parameters are constrained by the branching ratio of the decay $B \rightarrow X_s \gamma$. Even under these constraints, the value of x_s can be much different from the SM prediction.

The VQM incorporates extra quarks whose left-handed components, as well as right-handed ones, are singlets under the SU(2) gauge transformation. Then, the interactions of quarks become different from those in the SM. The Cabibbo-Kobayashi-Maskawa (CKM) matrix for the interactions with the W boson is extended and not unitary. The Z boson couples directly to the quarks with different flavors. The neutral Higgs boson also mediates flavor-changing interactions at the tree level.

Our study concentrates on $B_s\bar{B}_s$ mixing at the one-loop level through box diagrams. The contributions at the tree level have already been analyzed in the literature. The order of these tree-level diagrams is lower than the box diagrams of the SM. However, the experimental bounds on the branching ratio of the decay $B \rightarrow K \mu^+ \mu^-$ suggest very weak couplings for the flavor-changing interactions at the tree level. Consequently, the tree-level contributions turn out to be smaller than the one-loop contributions. On the other hand, the new box diagrams in the VQM are expected to contribute at the same order as those of the SM. Although these new contributions do not yield a drastic change from the SM prediction, precise measurements in near-future experiments, such as BTeV and the CERN Large Hadron Collider (LHCb), may be able to distinguish the VQM and the SM. Indeed, the VQM could give sizable new contributions to the decay $B \rightarrow X_s \gamma$ at the one-loop level [5], imposing non-trivial constraints on the model.

We assume, for definiteness, that there exist two vectorlike quarks U and D with electric charge $2/3$ and $-1/3$, respectively. The CKM matrix V is then enlarged to be a 4×4 matrix and expressed as

$$V_{ab} = \sum_{i=1}^3 (A_L^{u\dagger})_{ai} (A_L^d)_{ib}, \quad (1)$$

A_L^u and A_L^d being unitary matrices which diagonalize the mass matrices for up-type and down-type quarks, respectively. It should be noted that the matrix V is not unitary:

$$(V^\dagger V)_{ab} = \delta_{ab} - A_{L4a}^{d*} A_{L4b}^d. \quad (2)$$

The interaction Lagrangian for the quarks with the W and Goldstone bosons is given by

$$\begin{aligned} \mathcal{L} = & \frac{g}{\sqrt{2}} \sum_{a,b=1}^4 \bar{u}^a V_{ab} \gamma^\mu \frac{1-\gamma_5}{2} d^b W_\mu^\dagger \\ & + \frac{g}{\sqrt{2}} \sum_{a,b=1}^4 \bar{u}^a V_{ab} \left\{ \frac{m_{ua}}{M_W} \left(\frac{1-\gamma_5}{2} \right) - \frac{m_{db}}{M_W} \left(\frac{1+\gamma_5}{2} \right) \right\} d^b G^\dagger \\ & + \text{H.c.} \end{aligned} \quad (3)$$

Here, the mass eigenstates for the up-type and down-type quarks are denoted by u^a and d^b , a and b being the generation indices, and m_{ua} and m_{db} represent the corresponding mass eigenvalues. These eigenstates will also be denoted as (u, c, t, U) and (d, s, b, D) . The interaction Lagrangian for the down-type quarks with the Z , Higgs, and Goldstone bosons is given by

$$\begin{aligned} \mathcal{L} = & -\frac{g}{\cos \theta_W} \sum_{a,b=1}^4 \bar{d}^a \gamma^\mu \left\{ -\frac{1}{2} (V^\dagger V)_{ab} \frac{1-\gamma_5}{2} \right. \\ & \left. + \frac{1}{3} \sin^2 \theta_W \delta_{ab} \right\} d^b Z_\mu \\ & - \frac{g}{2} \sum_{a,b=1}^4 \bar{d}^a (V^\dagger V)_{ab} \left\{ \frac{m_{da}}{M_W} \left(\frac{1-\gamma_5}{2} \right) \right\} \end{aligned}$$

$$\begin{aligned}
& + \frac{m_{db}}{M_W} \left(\frac{1 + \gamma_5}{2} \right) \left. \right\} d^b H^0 \\
& + i \frac{g}{2} \sum_{a,b=1}^4 \bar{d}^a (V^\dagger V)_{ab} \left\{ \frac{m_{da}}{M_W} \left(\frac{1 - \gamma_5}{2} \right) \right. \\
& \left. - \frac{m_{db}}{M_W} \left(\frac{1 + \gamma_5}{2} \right) \right\} d^b G^0. \quad (4)
\end{aligned}$$

Since the matrix V is not unitary, there appear flavor-changing interactions at the tree level. The Lagrangians in Eqs. (3) and (4) contain also new sources of CP violation [6].

The amount of $B_s \bar{B}_s$ mixing is described by the mixing parameter x_s , which becomes

$$\begin{aligned}
x_s = & \frac{G_F}{3\sqrt{2}} (\sqrt{B_{B_s}} f_{B_s})^2 M_{B_s} \eta_{QCD} \tau_{B_s} \left| \{(V^\dagger V)_{23}\}^2 \right. \\
& \left. + \frac{G_F}{\sqrt{2}\pi^2} M_W^2 \sum_{a,b=1}^4 V_{a2}^* V_{a3} V_{b2}^* V_{b3} S(r_a, r_b) \right|, \quad (5)
\end{aligned}$$

$$\begin{aligned}
S(r_a, r_b) = & \frac{4 - 7r_a r_b}{4(1 - r_a)(1 - r_b)} + \frac{4 - 8r_b + r_a r_b}{4(1 - r_a)^2 (r_a - r_b)} r_a^2 \ln r_a \\
& + \frac{4 - 8r_a + r_a r_b}{4(1 - r_b)^2 (r_b - r_a)} r_b^2 \ln r_b, \quad (6)
\end{aligned}$$

with $r_a = m_{ud}^2 / M_W^2$. The first term in Eq. (5) comes from the diagram exchanging the Z boson at the tree level. The contribution from the tree-level diagram exchanging the Higgs boson is suppressed by a factor of $(m_b / M_W)^2$ and thus negligible.

The second term arises from the box diagrams. Neglecting the masses of the u and c quarks, we obtain

$$\begin{aligned}
& \sum_{a,b=1}^4 V_{a2}^* V_{a3} V_{b2}^* V_{b3} S(r_a, r_b) \\
& = \{(V^\dagger V)_{23}\}^2 + 2 \sum_{a=3,4} (V^\dagger V)_{23} V_{a2}^* V_{a3} I_1(r_a) \\
& + \sum_{a=3,4} (V_{a2}^* V_{a3})^2 I_2(r_a) + 2 V_{32}^* V_{33} V_{42}^* V_{43} I_3(r_3, r_4), \quad (7)
\end{aligned}$$

where the functions I_1 , I_2 , I_3 are defined by

$$I_1(r_a) = S(0, r_a) - S(0, 0), \quad (8)$$

$$I_2(r_a) = S(r_a, r_a) - 2S(0, r_a) + S(0, 0), \quad (9)$$

$$I_3(r_3, r_4) = S(r_3, r_4) - S(0, r_3) - S(0, r_4) + S(0, 0). \quad (10)$$

In our numerical calculations we take the bag factor B_{B_s} , the decay constant f_{B_s} , the meson mass M_{B_s} , and the meson lifetime τ_{B_s} for $\sqrt{B_{B_s}} f_{B_s} = 267$ MeV [7], $M_{B_s} = 5.37$ GeV, and $\tau_{B_s} = 1.49$ ps [8]. The QCD correction factor η_{QCD} is set at 0.55 [9].

The mixing parameter x_s depends on the U -quark mass m_U and the CKM matrix elements $V_{32}^* V_{33}$, $V_{42}^* V_{43}$, $(V^\dagger V)_{23}$. The mass should be larger than the top-quark mass. The matrix elements are related to V_{12} , V_{13} , V_{22} , and V_{23} which have been directly measured in experiments. Their experimental values [8] give a constraint

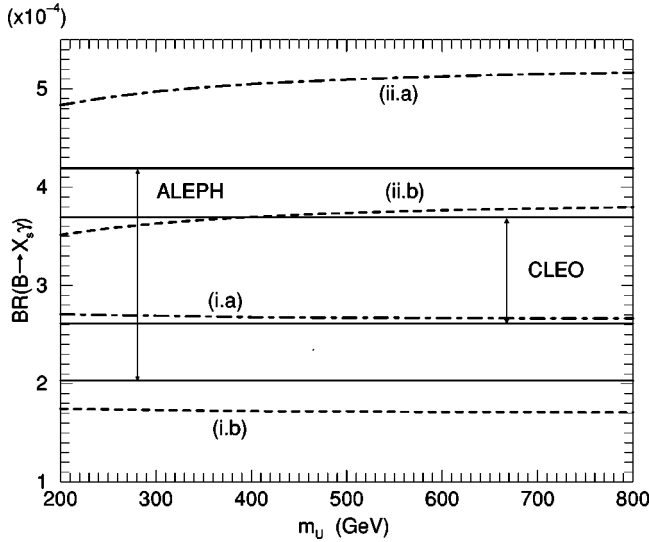


FIG. 1. The branching ratio of $B \rightarrow X_s \gamma$ for $V_{32}^* V_{33} = 0.035$ as a function of the U -quark mass. Four curves correspond to the four parameter sets given in Table I. The $1\text{-}\sigma$ allowed range of the branching ratio from CLEO [11] and ALEPH [12] are also shown.

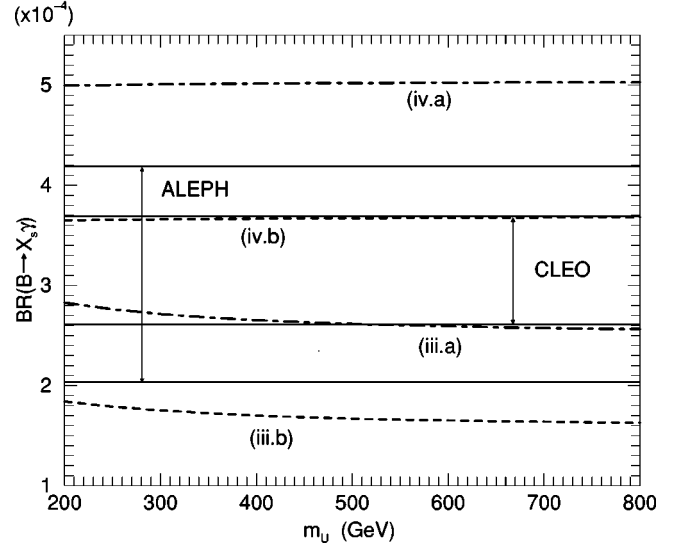


FIG. 2. The branching ratio of $B \rightarrow X_s \gamma$ for $V_{32}^* V_{33} = 0.045$ as a function of the U -quark mass. Four curves correspond to the four parameter sets given in Table II. The $1\text{-}\sigma$ allowed range of the branching ratio from CLEO [11] and ALEPH [12] are also shown.

TABLE I. The values of $V_{42}^*V_{43}$ and $(V^\dagger V)_{23}$ in Figs. 1 and 3.

	(i.a)	(i.b)	(ii.a)	(ii.b)
$V_{42}^*V_{43}$	-0.002	-0.002	0.010	0.010
$(V^\dagger V)_{23}$	-0.002	0.002	-0.002	0.002

$$0.03 < |V_{32}^*V_{33} + V_{42}^*V_{43} - (V^\dagger V)_{23}| < 0.05. \quad (11)$$

As seen in Eq. (4), the value of $(V^\dagger V)_{23}$ determines the flavor-changing interactions at the tree level. From the upper bounds on the branching ratio of the decay $B \rightarrow K\mu^+\mu^-$ [8], a constraint

$$|(V^\dagger V)_{23}| < 2.0 \times 10^{-3} \quad (12)$$

is derived.¹ The U -quark mass and the CKM matrix elements are related to each other through the mass matrices of the up-type and down-type quarks. However, there are many unknown factors for these mass matrices, leaving open various possibilities for the relations [10]. Therefore, for our numerical analyses, we assume that the model parameters m_U , $V_{32}^*V_{33}$, $V_{42}^*V_{43}$, and $(V^\dagger V)_{23}$ are independent of each other. For simplicity, these matrix elements are taken as real.

The model parameters are further constrained [5] from the branching ratio of $B \rightarrow X_s \gamma$, which has been measured by CLEO [11] and ALEPH [12] as, respectively, $Br(B \rightarrow X_s \gamma) = (3.15 \pm 0.35 \pm 0.32 \pm 0.26) \times 10^{-4}$ ($1-\sigma$) and $Br(B \rightarrow X_s \gamma) = (3.11 \pm 0.80 \pm 0.72) \times 10^{-4}$ ($1-\sigma$). We show its predicted branching ratio in Figs. 1 and 2 for $V_{32}^*V_{33} = 0.035$ and $V_{32}^*V_{33} = 0.045$, respectively, as a function of the U -quark mass. The values of $V_{42}^*V_{43}$ and $(V^\dagger V)_{23}$ are listed in Tables I and II. The experimental bounds are shown by solid lines. For $V_{32}^*V_{33} = 0.035$, the ranges $V_{42}^*V_{43} < -0.002$ and $0.010 < V_{42}^*V_{43}$ are not allowed from the CLEO bounds, irrespectively of the value for $(V^\dagger V)_{23}$. For $V_{32}^*V_{33} = 0.045$, similarly excluded are the ranges $V_{42}^*V_{43} < -0.011$ and $0.001 < V_{42}^*V_{43}$. The allowed ranges of $V_{42}^*V_{43}$ and $(V^\dagger V)_{23}$ do not depend very much on the U -quark mass. A rather large part of the region which satisfies Eqs. (11) and (12) becomes inconsistent with $B \rightarrow X_s \gamma$.

We now evaluate $B_s \bar{B}_s$ mixing within the obtained parameter ranges consistent with the experiments. In Figs. 3 and 4 the mixing parameter x_s is shown for the same parameter sets as those in Figs. 1 and 2, respectively. The solid line represents the SM prediction. The parameter x_s has a value

¹The present experimental bounds do not give non-trivial constraints on $V_{32}^*V_{33}$ and $V_{42}^*V_{43}$ which affect the decay through one-loop diagrams. For further discussions, see Ref. [13].

TABLE II. The values of $V_{42}^*V_{43}$ and $(V^\dagger V)_{23}$ in Figs. 2 and 4.

	(iii.a)	(iii.b)	(iv.a)	(iv.b)
$V_{42}^*V_{43}$	-0.011	-0.011	0.001	0.001
$(V^\dagger V)_{23}$	-0.002	0.002	-0.002	0.002

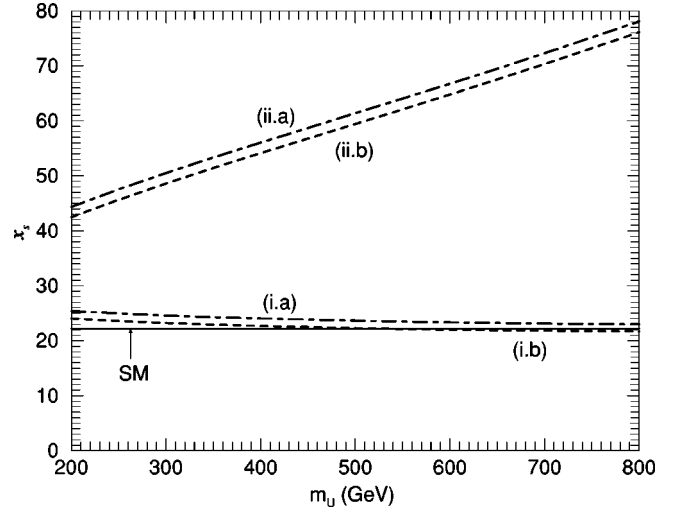


FIG. 3. The mixing parameter x_s for $V_{32}^*V_{33} = 0.035$ as a function of the U -quark mass. Four curves correspond to the four parameter sets given in Table I. The solid horizontal line represents the SM prediction for $m_t = 177$ GeV.

between the curves (i) and (ii) in Fig. 3 and the curves (iii) and (iv) in Fig. 4 for the ranges of $V_{42}^*V_{43}$ allowed by the CLEO bounds. A larger value for $V_{42}^*V_{43}$ leads to a larger value for x_s . For $V_{32}^*V_{33} = 0.035$ and $-0.002 \leq V_{42}^*V_{43} \leq 0.010$, the value of x_s is larger than the SM value, and their difference can be as much as a factor of 2 or more. As the value of $V_{32}^*V_{33}$ increases, this difference becomes small. Still, a deviation by a factor of 0.5 of the SM value can occur for $V_{32}^*V_{33} = 0.045$ and $-0.011 \leq V_{42}^*V_{43} \leq 0.001$. The value of $(V^\dagger V)_{23}$ does not affect much x_s , while a larger mass of the U quark tends to give a larger value for x_s . The magnitude of the tree-level contribution to x_s is at most 20% of the SM value. It should be noted that the value of x_s may be smaller than the SM value, which stands in contrast to the

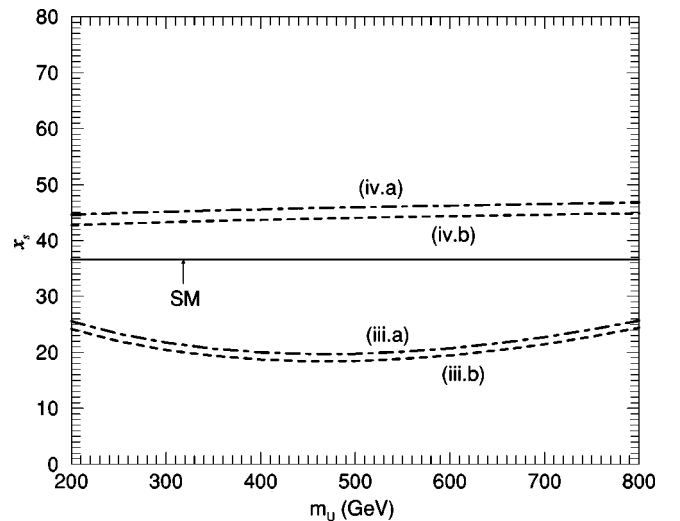


FIG. 4. The mixing parameter x_s for $V_{32}^*V_{33} = 0.045$ as a function of the U -quark mass. Four curves correspond to the four parameter sets given in Table II. The solid horizontal line represents the SM prediction for $m_t = 177$ GeV.

prediction by the supersymmetric standard model [3].

In the SM, the measurement of x_s determines the value of $V_{32}^*V_{33}$, which is examined from the point of unitarity for the CKM matrix. Within the present accuracies for the values of $V_{12}^*V_{13}$ and $V_{22}^*V_{23}$, the range $x_s > 50$ leads to unitarity violation. More precise measurements of $V_{12}^*V_{13}$ and $V_{22}^*V_{23}$, together with smaller errors in calculating B_{B_s} and f_{B_s} , will make it possible to examine the range $x_s < 50$. Alternatively, the value of $V_{32}^*V_{33}$ may be compared with that measured by the top-quark decays. A possible contradiction in these examinations within the framework of the SM could imply the existence of the vector-like quarks.

In summary, we have studied the effects of the VQM on $B_s\bar{B}_s$ mixing. The contribution of the W -mediated diagrams

at the one-loop level could be sizably different from that in the SM. On the other hand, the Z -mediated diagrams at the tree level cause merely a small effect. The VQM is constrained from experimental results for the radiative decay $B \rightarrow X_s \gamma$. Under these constraints, the mixing parameter x_s can non-trivially be larger or smaller than the SM prediction. Its value could be more than twice the SM value. The measurement of x_s provides a useful test for the VQM.

The authors thank T. Onogi and M. Yamauchi for discussions. The work of M.A. is supported in part by a Grant-in-Aid for Scientific Research from the Ministry of Education, Science and Culture, Japan. M.A. thanks the JSPS for financial support.

-
- [1] For reviews, see P.J. Franzini, Phys. Rep. **173**, 1 (1989); Y. Nir and H.R. Quinn, Annu. Rev. Nucl. Part. Sci. **42**, 211 (1992).
- [2] N. Oshimo, Nucl. Phys. **B404**, 20 (1993).
- [3] G.C. Branco, G.C. Cho, Y. Kizukuri, and N. Oshimo, Phys. Lett. B **337**, 316 (1994); Nucl. Phys. **B449**, 483 (1995).
- [4] Y. Nir and D. Silverman, Phys. Rev. D **42**, 1477 (1990); D. Silverman, *ibid.* **45**, 1800 (1992); G.C. Branco, T. Morozumi, P.A. Parada, and M.N. Rebelo, *ibid.* **48**, 1167 (1993); K. Fujikawa, Prog. Theor. Phys. **92**, 1149 (1994); G. Bhattacharyya, G.C. Branco, and D. Choudhury, Phys. Lett. B **336**, 487 (1994); V. Barger, M.S. Berger, and R.J.N. Phillips, Phys. Rev. D **52**, 1663 (1995); L.T. Handoko and T. Morozumi, Mod. Phys. Lett. A **10**, 309 (1995); **10**, 1733(E) (1995); C.-H.V. Chang, D. Chang, and W.-Y. Keung, Phys. Rev. D **61**, 053007 (2000).
- [5] M. Aoki, E. Asakawa, M. Nagashima, N. Oshimo, and A. Sugamoto, Phys. Lett. B **487**, 321 (2000).
- [6] E. Asakawa, M. Marui, N. Oshimo, T. Saito, and A. Sugamoto, Eur. Phys. J. C **10**, 327 (1999).
- [7] C. Bernard, hep-lat/0011064.
- [8] Particle Data Group, D. Groom *et al.*, Eur. Phys. J. C **15**, 1 (2000).
- [9] A.J. Buras and R. Fleischer, *Heavy Flavours II* (World Scientific, Singapore, 1998), p. 65.
- [10] See, e.g., K. Higuchi and K. Yamamoto, Phys. Rev. D **62**, 073005 (2000).
- [11] CLEO Collaboration, S. Ahmed *et al.*, CLEO CONF 99-10 (1999).
- [12] ALEPH Collaboration, R. Barate *et al.*, Phys. Lett. B **429**, 169 (1998).
- [13] M.R. Ahmady, M. Nagashima, and A. Sugamoto, Phys. Rev. D **64**, 054011 (2001).